Cw mode-locked deep UV pulses at an average power of 1.8 W

2000 J. Opt. A: Pure Appl. Opt. 2 L41

(http://iopscience.iop.org/1464-4258/2/6/101)

J. Opt. A: Pure Appl. Opt. **2** (2000) L41–L43. Printed in the UK PII: S1464-4258(00)14061-9

LETTER TO THE EDITOR

Cw mode-locked deep UV pulses at an average power of 1.8 W

J C Garcia†, A K Newman†, J M Liu† and M C Lee‡

† Department of Electrical Engineering, University of California at Los Angeles, Los Angeles, CA 90095, USA
‡ Department of Electrophysics, National Chiao Tung University, Hsin Chu, Taiwan, Republic of China

Received 19 May 2000, in final form 11 August 2000

Abstract. We report a cw mode-locked train of ∼3.6 ps deep UV pulses with an average power of up to 1.8 W at 263 nm. This UV source is the result of two-stage, single-pass fourth-harmonic generation of an additive-pulse mode-locked Nd:YLF laser using KTP and BBO crystals. Conversion efficiencies of up to 47% from 1.053 μm to 527 nm and up to 39% from 527 to 263 nm have been observed.

Keywords: Nonlinear optics, frequency conversion, second-harmonic generation, fourth-harmonic generation

Typically, ultraviolet sources at wavelengths shorter than 300 nm with average powers measured in watts have been achieved with giant pulse systems at kilohertz repetition rates [1]. With the increased importance of UV sources for a wide range of applications such as machining, spectroscopy and biomedical research, there is a need for high-power cw and quasi-cw UV sources. Resonant-ring systems have demonstrated efficiencies as high as 24% in the conversion of IR to UV, resulting in average powers of up to 3.5 W for cw mode-locked systems [2, 3] and 1.5 W for a true cw laser [4]. In this letter we report a system capable of comparable conversion efficiencies without the benefit of a resonant ring. This system uses an additive-pulse mode-locked (APM) Nd:YLF laser [5] at 1.053 μm with an average power of 10.4 W. The uniqueness of this APM laser is that it generates IR pulses of width 6.1 ps with a repetition rate of 76 MHz. The resulting second-harmonic generation (SHG) efficiencies, of the order of 50 and 40% for conversion of 1.053 μm to 527 nm and 527–263 nm respectively, yield a cw mode-locked train of ∼3.6 ps, deep UV pulses at 263 nm wavelength with measured average power of up to 1.8 W. This results in a total IR-to-UV fourth-harmonic conversion efficiency of 17%.

Figure 1 shows the experimental setup. The 1.053 μm output of the flash-lamp pumped APM Nd:YLF laser passes through an attenuator, comprised of an IR half-wave plate and a beamsplitter polarizer. This setup allows us to vary IR input power without affecting the characteristics of the original source. The output of the attenuator passes through a second IR half-wave plate and a 10 cm lens that focuses it into a 5 mm long KTP crystal cut in the x–y plane for type II SHG. A second 10 cm lens positioned after the KTP crystal collimates the 527 nm, second-harmonic beam. The

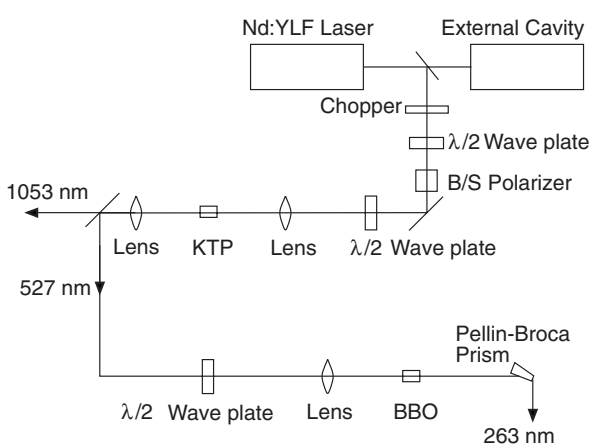

Figure 1. Experimental setup.

IR and second harmonic are separated by two 45° harmonic separators each reflecting more than 99% of incident 527 nm light and transmitting more than 90% of incident IR. The resulting second-harmonic beam passes through a half-wave plate for the 527 nm wavelength and then through a 20 cm lens that focuses it into a 7 mm long BBO crystal cut for type I SHG. A Pellin Broca prism separates the unconverted 527 nm light from the UV and delivers the UV beam to a Newport 818T-10 power meter.

Figure 2 shows the 1.053 μm to 527 nm conversion efficiency versus the input 1.053 μm fundamental power. We achieved a maximum efficiency of 47%. The two curves represent different crystal orientations relative to the spatial profile of the IR beam. The IR beam has a slight elongation in its spatial profile which results in different conversion

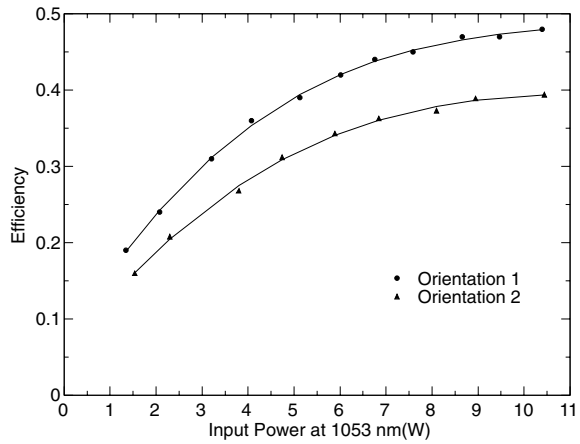

Figure 2. SHG efficiency for converting the IR at 1.053 μm to 527 nm. For orientation 1, a maximum efficiency of 47% was achieved, corresponding to the generation of 4.9 W of 527 nm light with 10.4 W of IR input power. For orientation 2, a maximum efficiency of 39% was achieved, corresponding to the generation of 4.1 W of 527 nm light with 10.4 W of IR input power.

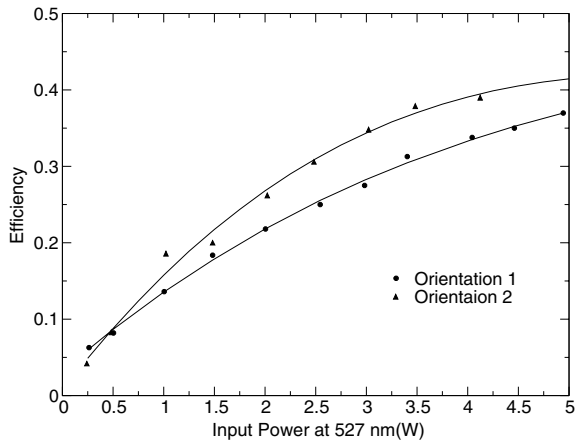

Figure 3. SHG efficiency for converting 527 nm to UV at 263 nm. For orientation 1, a maximum efficiency of 37% was achieved, corresponding to the generation of 1.8 W of UV with 4.9 W of 527 nm input power. For orientation 2, a maximum efficiency of 39% was achieved, corresponding to the generation of 1.6 W of UV with 4.1 W of 527 nm input power.

efficiencies when the nonlinear crystals are rotated by 90° around the beam axis. In orientation 1, the phase matching axis for the KTP crystal is along the elongated axis of the fundamental beam, and that for the BBO crystal, is 90° from the elongated axis of the fundamental beam. In orientation 2, both nonlinear crystals are rotated by 90° around the beam axis relative to orientation 1. Figure 3 shows the 527–263 nm efficiency curves for each of the aforementioned orientations. The maximum 527–263 nm efficiency is 39% in orientation 2. Unfortunately the orientations for the maximum conversion efficiencies do not correspond to one another. Eventually this could be corrected by a combination of cylindrical and spherical lenses. Combining the maximum efficiencies of both stages of SHG, it is apparent that upwards of 2 W of UV average power could be generated. In addition, the maximum realized intensity in the BBO crystal is well below the reported damage threshold [6]. Higher intensities in the BBO, while compensating for the phase matching condition, could allow the power to be pushed higher. We could not similarly improve 1.053 μm to 527 nm efficiency as we were on the verge of damaging the KTP crystal in the current configuration. It should be noted that in orientation 1, because the UV beam is s-polarized relative to the input and output surfaces of the Pellin Broca Brewster angle prism, approximately 14% of the UV power is lost at each surface. We were able to measure the reflected beam from the input surface along with the transmitted beam through both surfaces. The reflected power from the output surface was calculated and included in the reported values. In orientation 2, the UV beam is p-polarized relative to the prism and is nearly fully transmitted at both the input and output surfaces. This is clearly a more desirable orientation, as nearly all of the UV power is in a single beam. In addition, 527–263 nm conversion efficiency is higher in this orientation.

Figures 4 and 5 show the optical spectra of the UV and 527 nm beams, respectively. The spectra were measured using a McPherson 0.67 m monochromator with a resolution of 0.06 nm. The measured full width at half maximum

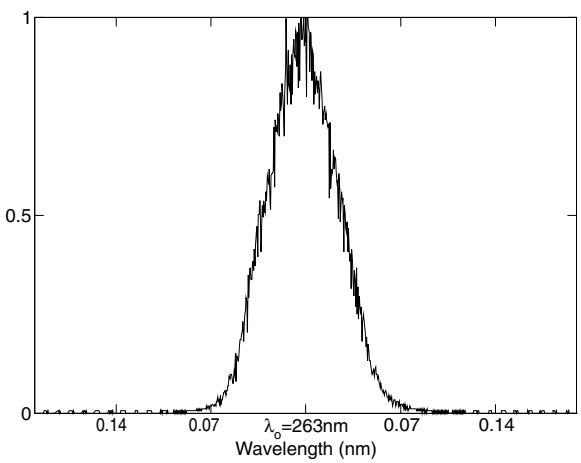

Figure 4. Spectrum of the UV pulses at 263 nm. The FWHM of 0.06 nm is limited by the resolution of the monochromator.

(FWHM) of the UV spectrum is 0.06 nm, which is equal to the resolution of the monochromator. Based on the 527 nm measured spectral width of 0.13 nm, the theoretically expected FWHM of the UV spectrum, 0.046 nm, is slightly narrower than the resolution of the monochromator. As our measured UV spectrum is at the limit of the resolution of the monochromator, the true spectral width of the UV pulses could be narrower than 0.06 nm.

We could not directly measure the UV pulse width using our autocorrelator because there is no suitable nonlinear crystal for SHG of the UV pulses at 263 nm wavelength. The UV pulse width had to be estimated based upon the measured 527 nm pulse width and the assumption of an ideal SHG process. The measured 527 nm pulse width was 5.1 ps FWHM. The autocorrelation trace, shown in figure 6, was measured using a Femtochrome FR-103 autocorrelator with a BBO crystal. We assume a hyperbolic secant squared pulse shape. The time–bandwidth product of the 527 nm pulse is 0.72, which is approximately twice the transform limit. Based on this 527 nm pulse width, the UV pulse

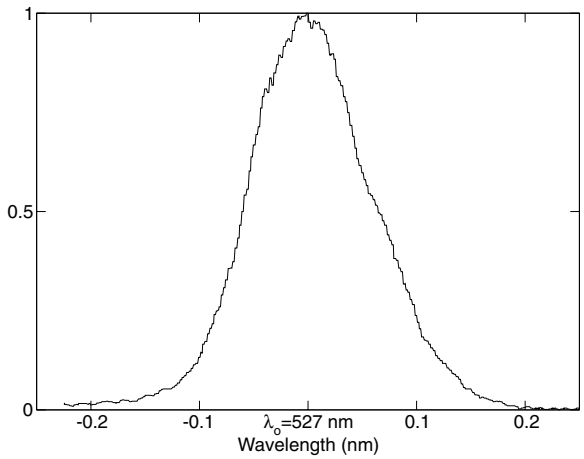

Figure 5. Spectrum of the second-harmonic pulses at 527 nm with an FWHM of 0.13 nm.

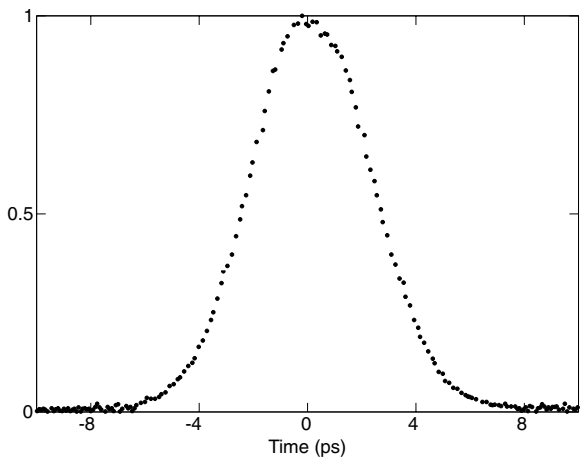

Figure 6. Autocorrelation trace for the pulses at 527 nm. The FWHM pulse width is 5.1 ps assuming a hyperbolic secant squared pulse shape.

width is estimated to be 3.6 ps FWHM, yielding a time–bandwidth product of 0.94, as limited by the resolution of the monochromator.

The spatial profile of the UV beam displays the same elongated shape as seen in previous experiments [7, 8] due to the phase matching conditions in the BBO. In the near field, the elongated dimension of the beam is along the critical phase matching axis. It will be necessary to use a combination of cylindrical and spherical lenses to ultimately achieve a circularly symmetric far-field spatial profile.

At the high end of the efficiency curves shown in figures 2 and 3, the thermal effect due to the high average power delivered to both the KTP and BBO crystals caused the phase matching angles to require adjustment. Because of the resulting difficulty in optimizing the phase matching angles, an optical chopper with a 2 : 1 duty cycle was inserted into the setup as shown in figure 1. Prior to the insertion of the chopper, the phase matching angles had to be optimized at IR power levels exceeding 7 W to prevent conversion efficiencies from deteriorating. After inserting the chopper, the duty cycle was reduced to 50%, which significantly reduced the necessary adjustments to the phase matching angles for both crystals. It is our intention to further investigate these thermal effects on the second-harmonic processes in KTP and BBO.

This laser has proven to be a reliable and stable system for producing UV light. As indicated earlier, the laser intensity in the BBO crystal is below the damage threshold of the crystal. Damage to the BBO crystal has not been an issue and in no way has it limited the reliability of the nonlinear process. Heating of the crystal is not a limiting factor either, though it causes the phase matching angles to require fine adjustments as discussed earlier. The laser can be operated for hours at full power without any noticeable change in the efficiency [5]. In addition, the intensity in the BBO crystal can still be further increased to achieve higher conversion efficiencies. Using a pair of cylindrical lenses, the focusing could be better matched to the acceptance angles for each of the the two axes, providing better phase matching conditions than using a single spherical lens as in the case reported in this letter.

There are many potential applications for the high-average-power, picosecond UV pulses reported in this letter. We have already begun to use this system for photoluminescence studies of high-energy transitions in large-bandgap semiconductor materials such as GaN. With an average power of 1.8 W and a pulse width of ∼3.6 ps we expect this UV source to exceed the threshold for a synchronously pumped optical parametric oscillator to generate tunable visible and UV radiation [9,10]. Additionally this system could potentially be used for time resolved spectroscopy and micro-machining [11].

References

[1] Kojima T, Konno S, Fujikawa S, Yasui K, Yoshizawa K, Mori Y, Sasaki T, Tanaka M and Okada Y 2000 20-W ultraviolet-beam generation by fourth-harmonic generation of an all-solid-state laser *Opt. Lett.* **25** 58–60

[2] Kuczewski A J, Thorn C E, Matone G and Giordano G 1999 Production of high-power CW UV by resonant frequency quadrupling of a Nd:YLF laser *Proc. SPIE* **3610** 57–68

[3] Tidwell S C, Seamans J F and Lowenthal D D 1993 Efficient high-power UV generation by use of a resonant ring driven by a cw mode-locked IR laser *Opt. Lett.* **18** 1517–9

[4] Oka M, Liu L Y, Wiechmann W, Eguchi N and Kubota S Piper 1995 All solid-state continuous-wave frequency-quadrupled Nd:YAG laser *IEEE J. Sel. Topics Quantum Electron.* **1** 859–66

[5] Liu J M and Chee J K 1990 Passive mode locking of a cw Nd:YLF laser with a nonlinear external coupled cavity *Opt. Lett.* **15** 685–7

[6] Borsutzky A, Brunger R, Huang Ch and Wallenstein R 1991 Harmonic and sum-frequency generation of pulsed laser radiation in BBO, LBO, and KD*P *Appl. Phys.* B **52** 55–62

[7] Persaud M A, Tolchard J M and Ferguson A I 1990 Efficent generation of picosecond pulses at 243 nm *IEEE J. Quantum Electron.* **26** 1253–8

[8] Kuroda K, Omatsu T, Shimura T, Chihara M and Ogura I 1990 Second harmonic generation of a copper vapor laser in barium borate *Opt. Commun.* **75** 42–6

[9] Tang Y, Cui Y and Dunn M H 1992 Lithium triborate optical parametric oscillator pumped at 266 nm *Opt. Lett.* **17** 192–4

[10] Hanson F 1989 Blue parametric generation from temperature-tuned LBO *Opt. Lett.* **4** 205–7

[11] Glover A C, Illy E and Piper J 1995 High-speed UV micro-machining of polymers with frequency-doubled copper vapor lasers *IEEE J. Sel. Topics Quantum Electron.* **1** 830–6